

Electrocardiographic characteristics for successful radiofrequency ablation of right coronary cusp premature ventricular contractions

Sung Il Im, MD^a, Sung Ho Lee, MD^b, Hye Bin Gwag, MD^c, Youngjun Park, MD^c, Seung-Jung Park, MD^c, June Soo Kim, MD^c, Young Keun On, MD^c, Kyoung-Min Park, MD^{c,*}

Abstract

Electrocardiographic (ECG) criteria identifying right- and left-sided outflow tract origins have been established. The purpose of this study was to define the criteria for premature ventricular contractions (PVCs) originating from the right coronary cusp (RCC) adequately.

We analyzed ECG and electrophysiologic study data from patients who underwent successful ablation of PVCs originating from the RCC and right ventricular outflow tract (RVOT). Eighteen RCC and 28 septal RVOT PVCs were studied. Among these 18 successful RCC PVCs, a predominantly positive QRS in lead I in 18/18 (100%), longer V_{1-2} R-wave duration (81.4 ± 31.1 vs 44.8 ± 7.0 ms, $P = .02$), V_{1-2} R wave duration index (RWDI) (51.3 ± 22.0 vs $31.2 \pm 7.5\%$, $P = .06$) were observed compared to those with posteroseptal RVOT. Local ventricular activation time preceding QRS onset was significantly earlier (-38 ± 12 ms) at the successful RCC ablation site compared to the failed ablation site of the septal RVOT (-22 ± 8 ms), even without good pace mapping at the RVOT ($P < .001$). The receiver operating characteristic curve showed that a pre-QRS time of ≥ -31 ms predicted successful RCC ablation with 67% sensitivity and 94% specificity. A predominantly positive QRS in lead I, longer R-wave duration and RWDI in lead V_1 or V_2 with a local ventricular activation preceding QRS onset by an average of -31 ms suggests an effective RCC ablation site.

Abbreviations: AF = atrial fibrillation, ASOV = aortic sinuses of Valsalva, ECG = electrocardiography, EF = ejection fraction, HR = heart rate, ICE = intracardiac echocardiography, LCC = left coronary cusp, MDI = maximum deflection index, NCC = non-coronary cusp, NSR = normal sinus rhythm, PACs = premature atrial contractions, PVCs = premature ventricular contractions, RCC = right coronary cusp, RF = radiofrequency, RSWAI = R/S-wave amplitude index, RSWAR = R/S-wave amplitude ratio, RVOC = right ventricular outflow tract, RWDI = R wave duration index, sRVOT-a = anteroseptal RVOT, sRVOT-p = posteroseptal RVOT, TTE = transthoracic echocardiogram, VAs = ventricular arrhythmias.

Keywords: electrocardiogram, premature ventricular contraction, right coronary cusp

1. Introduction

Premature ventricular contractions (PVCs) arising from the aortic sinuses of Valsalva (ASOV) account for up to 21% of idiopathic

PVCs.^[1] These arrhythmias commonly arise from the left coronary cusp (LCC) and right coronary cusp (RCC) and rarely from the non-coronary cusp (NCC).^[2,3] This arrhythmogenicity was thought to be related to myocardial extensions projecting above the aortic valve into the ASOV. Ouyang et al^[2] suggested that R-wave duration and R/S-wave amplitude indices in leads V_1 and V_2 could be used to differentiate the RCC and right ventricular outflow tract (RVOT). Lin et al^[4] presented 12-lead electrocardiographic (ECG) characteristics of the right cusp lesion, guided by intracardiac echocardiography (ICE) and electroanatomic mapping, summarized as a QR or Qr in V_1 , small broad R-wave in V_2 , and variable precordial transition. They also described RCC PVCs as difficult to differentiate due to the close anatomic relationship between the RCC and RVOT. Yamada et al^[5,6] reported that 25% of patients who underwent evaluation of aortic root ventricular arrhythmias (VAs) had localized preferential breakout sites in the RVOT. The mechanism of this preferential conduction may be explained by anisotropic conduction between the aortic root origin and breakout site in the RVOT.^[5-9] However, there was limited data about ECG and electrophysiological characteristics of RCC PVCs considering their anatomical relationship to the septal RVOT in order to successfully guide ablation procedures. In this study, we sought to determine the electrocardiographic and ablation procedural characteristics of RCC PVCs to guide successful RF ablation.

Editor: Simone Gulletta.

The authors have no conflicts of interest to declare.

^aDivision of Cardiology, Department of Internal Medicine, Kosin University Gospel Hospital, Kosin University College of Medicine, Busan, ^bDivision of Cardiology, Department of Internal Medicine, Kangbuk Samsung Hospital, ^cDivision of Cardiology, Department of Internal Medicine, Samsung Medical Center, Sungkyunkwan university School of Medicine, Seoul, Republic of Korea.

* Correspondence: Kyoung-Min Park, Division of Cardiology, Heart Vascular Stroke Institute, Samsung Medical Center, Sungkyunkwan university School of Medicine, 81 Irwon-ro, Gangnam-gu, Seoul 06351, Republic of Korea (e-mail: kyoungmin.park@samsung.com).

Copyright © 2020 the Author(s). Published by Wolters Kluwer Health, Inc. This is an open access article distributed under the terms of the Creative Commons Attribution-Non Commercial License 4.0 (CCBY-NC), where it is permissible to download, share, remix, transform, and buildup the work provided it is properly cited. The work cannot be used commercially without permission from the journal.

How to cite this article: Im SI, Lee SH, Gwag HB, Park Y, Park SJ, Kim JS, On YK, Park KM. Electrocardiographic characteristics for successful radiofrequency ablation of right coronary cusp premature ventricular contractions. *Medicine* 2020;99:11(e19398).

Received: 5 November 2019 / Received in final form: 23 January 2020 /

Accepted: 3 February 2020

<http://dx.doi.org/10.1097/MD.00000000000019398>

2. Methods

2.1. Study population

All patients enrolled in this study were diagnosed with frequent PVCs without known heart disease and underwent successful PVC ablation at the Samsung Medical Center in Korea between January 1, 2010 and December 31, 2017. This study complied with the Declaration of Helsinki, and the research protocol was approved by the ethics committee of Samsung Medical Center. We retrospectively analyzed consecutive patients with structurally normal hearts who were referred to our institution for catheter ablation. Patients had frequent idiopathic PVCs located in the right aortic cusp and septal RVOT and a PVC burden of >10,000 PVCs per 24 hours. Successful ablation was defined as at least an 80% reduction in the 24-hour PVC burden, based on our previously published experience.^[10] Active ischemia or a prior infarction causing cardiomyopathy were ruled out by the patients history and either coronary angiography or stress testing. Structurally normal hearts were defined by a normal nuclear perfusion scan, normal transthoracic echocardiogram (TTE), and/or normal coronary angiography. Cardiac catheterization was performed due to equivocal perfusion scans in 4 patients who had normal coronary angiograms. The right coronary cusp regions were defined as anterior, middle, and posterior. The RVOT regions were defined as anteroseptal RVOT (sRVOT-a) and RVOT

RVOT (sRVOT-p) sites. ICE and fluoroscopic guidance were used to define these specific regions. Fluoroscopic guidance was used to define the directions of the RVOT region. Beta-blockers, calcium channel blockers, and antiarrhythmic medications were discontinued for 5 half-lives before the study.

2.2. Assessment of preprocedural PVC burden and LV function

Twenty four hour Holter monitoring was performed to assess PVC burden at baseline. All patients underwent echocardiography prior to ablation to assess LV systolic function and diameter. The ejection fraction (EF) was calculated using Simpson formula.

2.3. Mapping and RF catheter ablation

Patients were brought to the electrophysiology laboratory in a postabsorptive, non-sedated state after written informed consent had been obtained in accordance with the Samsung Medical Center institutional guidelines. The RVOT was initially mapped with a 7 Fr, 4-mm tip NaviStar catheter placed in the right femoral vein. Detailed activation and pace mapping were performed in the RVOT, and sinus rhythm electrograms were analyzed. If a diffuse activation pattern was noted on the three-dimensional electroanatomic map (CARTO, Biosense Webster, Diamond Bar, CA, USA) and/or pace mapping resulted in a poor pace map match, attention was turned to the LVOT region. Intravenous heparin was administered to maintain an activated clotting time of >250 seconds during aortic cusp and/or LV endocardial mapping. An electroanatomic shell of the aortic cusp region was created. The mapping catheter was located on ICE, and pace mapping was performed at the threshold output from multiple sites in each cusp and from the RCC/LCC junction. The location of each pacing site was tagged on the electroanatomic map. Detailed activation mapping during VAs was performed in the aortic cusp region, and the earliest area of activation was

marked on the electroanatomic map and confirmed on ICE. Radiofrequency (RF) applications were applied to the site that exhibited the earliest bipolar activity during PVCs with a target temperature of 50°C and starting power of 20 W with gradual titration to a maximum power of 50 W. If PVC termination occurred in the first 10 seconds, RF delivery typically was continued for an additional 30 seconds. If termination did not occur in the first 10 to 15 seconds of RF delivery, RF delivery was terminated and the catheter was repositioned. RF ablation was first performed with a standard, 4-mm, non-irrigated catheter. An irrigated catheter was used only if a standard 4-mm tip catheter delivered inadequate power. The maximum power delivery was 30 W with the irrigated ablation catheter. Successful catheter ablation was defined as absence of spontaneous or inducible PVCs with an isoproterenol infusion (2–20 µg) and burst pacing from the RV apex or high right atrium for 30 to 60 minutes after RF ablation of the final lesion.

2.4. ECG measurements

The sinus rhythm and PVC ECG morphologies were measured on the same 12-lead ECG with electronic calipers on the Prucka CardioLab recording system (GE Healthcare, Waukesha, WI, USA). Standard 12-lead ECG electrode placement was used. The lead gain was uniform with a paper speed of 100 mm/s. During clinical PVCs, the following measurements were obtained during both sinus rhythm and PVC:

1. lead I vector and s-wave amplitude (ms),
2. leads II and III R-wave amplitude (mV) and II/III ratio,
3. leads aV_L and aV_R S-wave amplitude (mV) and aV_R/aV_L ratio,
4. total QRS duration (ms),
5. V₁₋₂ R-wave duration (ms),
6. V₁₋₂ R-wave duration index (RWDI, %),
7. R/S-wave amplitude ratio (RSWAR) in leads V₁ and V₂,
8. V₁₋₂ R/S-wave amplitude index (RSWAI, %),
9. maximum deflection index (MDI), and
10. V₂ transition ratio.

The following ECG patterns were investigated:

1. bundle branch block pattern and
2. precordial R-wave transition with PVCs and normal sinus beats.

The T–P segment was considered an isoelectric baseline for measurement of the R- and S-wave amplitudes. The QRS duration was measured from the site of the earliest initial deflection at the isoelectric line in any lead to the time of the last activation in any lead. The R-wave duration in leads V₁ and V₂ was determined from the onset of the QRS complex to the transition point between the R-wave and isoelectric line. The R-wave duration index was calculated as a percentage by dividing the QRS complex duration by the longest R-wave duration in lead V₁ or V₂. The R/S-wave amplitude ratio in leads V₁ and V₂ was measured from the QRS complex peak or nadir to the isoelectric line, and was expressed as a percentage. The R/S-wave amplitude index was then calculated from the greatest percentage of the R/S-wave amplitude ratio in lead V₁ or V₂. The MDI was calculated by dividing the shortest time to maximum deflection in any precordial lead by the QRS duration. The transition ratio was calculated in lead V₂ by computing the percentage of the R-wave during PVCs (R-wave/R-wave + S-wave) divided by the

percentage of the R-wave in normal sinus rhythm (NSR) (R-wave/R-wave + S-wave).^[11]

2.5. Electrophysiologic parameters during mapping and RF ablation

We reviewed the Prucka records and electrophysiology reports of 18 RCC patients and evaluated the various parameters listed below during pace mapping and RF ablation:

1. Pre-QRS time: interval from the earliest signal on the ablation catheter to the earliest QRS during clinical PVC (Fig. 1)
2. Pre-potential: any evidence of a pre-QRS potential-like signal
3. Late potential-sinus rhythm (SR): any evidence of a potential-like signal post-QRS
4. His bundle potential-SR: evidence of His potential on the distal ablation catheter at the successful ablation site
5. Pace map score: a comparison score was divided into either perfect or poor according to ECG analysis of the morphologies in each lead using PASO algorithm (3D CARTO system, Johnson & Johnson company):
 - Excellent - if the PVC and paced QRS complex were identical or very similar in all 12 lead tracings
 - Good - no differences in the bundle branch block morphology and frontal plane axis and very similar in 10 or 11 of the 12 lead tracings
 - Poor - if the PVC and paced QRS complex were identical or very similar in only 9 of the 12 lead tracings
 - Bad - if the PVC and paced QRS complex were identical or very similar in less than 9 of the 12 lead tracings
6. Number of RF lesions: total effective (>30seconds) lesion numbers at each site
7. Successful ablation sites within the RCC: we divided the sites into 3 categories (anterior, middle, and posterior) via intracardiac ECG analysis

2.6. Follow-up

All patients underwent 24-hour full-disclosure telemetry monitoring immediately following the procedure. TTE was performed

the day after the procedure to assess any structural changes and to confirm whether the LVEF change in the absence of PVCs occurred or not. The majority of patients were followed up in our Arrhythmia Center with routine ECG at 6 weeks and a follow-up ECG 4–12 months after ablation. For patients not followed at the Samsung Medical Center, the referring cardiologists were contacted and the medical records reviewed. All patients had a follow-up echocardiogram 3 to 12 months postablation. The arrhythmia burden was assessed by symptoms, ECG, and Holter monitoring. During the follow-up, 4 patients in RCC group and 3 patients in RVOT group had beta blockers due to LV dysfunction for 3 months. However, after LVEF recovery, those patients stopped beta blockers.

2.7. Statistical analysis

Descriptive data were presented as the mean ± SD or median (range). Between-group comparisons were made using a Student *t* test, whereas within-group comparisons were achieved using paired *t* tests. Characteristics of the RCC, sRVOT-p, and sRVOT-a sites were compared using analysis of variance (ANOVA) to assess the overall difference among the groups. Bonferroni correction was used to correct for multiple comparisons within groups. Characteristics of the RCC and sRVOT-p between 2 groups were assessed with the independent *t*-test. Receiver operating characteristic (ROC) analysis was performed to evaluate the optimal cut-off value of the pre-QRS time for successful RF ablation in the RCC. SPSS Version 16.0 for Windows software (SPSS Inc., Chicago, IL, USA) was employed for analysis. The difference was considered significant at *P* < .05.

3. Results

Among 96 consecutive patients at our institutions with frequent PVCs from January 2010 to December 2017, 46 patients (24 men; mean age 47 ± 15 years) who underwent successful ablation in the RCC or septal RVOT were enrolled in this study. Of these, 18 patients had RCC PVCs and 28 had PVCs from septal sites of the RVOT (sRVOT) (8 anterior and 20 posterior). The acute procedural success rate, defined as the absence of observed targeted PVCs during at least a 30 minutes period after the ablation, was achieved in 46 of the 46 (100%) patients in the study population. The long-term success rate, defined as at least an 80% reduction in the PVC burden on postprocedural Holter monitoring, was 90%. Ten percent (5/46) required a second procedure (performed at our institution) to achieve successful ablation. Postprocedure Holter monitoring was performed at a median of 3.6 months. The mean follow-up period after successful ablation was 33.3 ± 14.7 months, and there were no significant differences between the groups (31 ± 12, 29 ± 15, and 35 ± 16 months for RCC, sRVOT-p, and sRVOT-a, respectively, *P* = .45).

3.1. Baseline characteristics of the RCC and sRVOT site groups

Baseline characteristics of the RCC and sRVOT site groups are shown at Table 1. There were no significant differences in age between the 3 groups (*P* = .31). There were more male patients in the RCC PVC group than the sRVOT group (*P* = .004). Initial LVEF (%) and body surface area did not differ significantly between the groups (*P* = .50 and *P* = .17, respectively). The

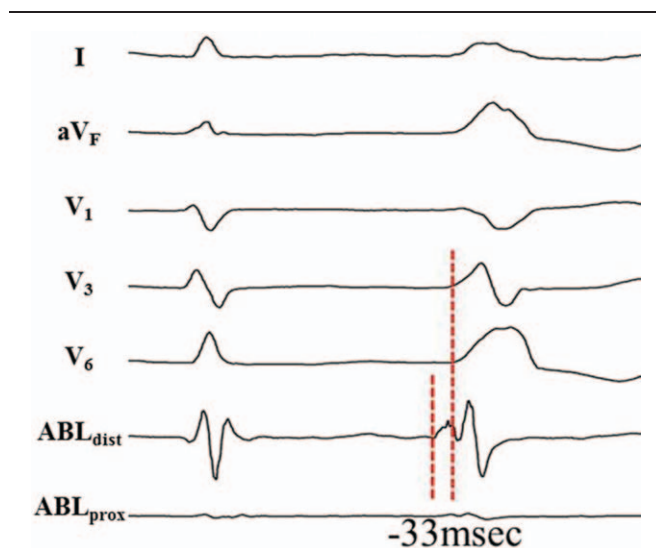


Figure 1. Pre-QRS time: interval from earliest signal on the ablation catheter to earliest QRS during the clinical PVC. PVC, premature ventricular contraction.

Table 1
Baseline characteristics of PVCs, according to the site of origin.

	RCC (n = 18)	sRVOT-p (n = 20)	sRVOT-a (n = 8)	P value	P value*
Male	15 (83.3)	8 (40.0)	3 (37.5)	.004	.09
Age (years)	51 ± 16	42 ± 18	44 ± 13	.31	.29
LVEF (%)	49.3 ± 11.3	49.0 ± 24.8	54.3 ± 12.6	.50	.97
BSA (m ²)	2.1 ± 0.2	1.9 ± 0.2	1.9 ± 0.2	.17	.19
QRS axis	20.6 ± 33.9	22.6 ± 32.6	34.4 ± 32.2	.45	.91
AAD drugs (%)	21	20	25	.85	.92
PVC burden (%/24 hour)	23.8 ± 12.1	13.5 ± 13.7	23.2 ± 15.0	.41	.18
PVC burden (n/24 hrs)	25,308 ± 14,020	17,308 ± 12,585	19,656 ± 16,479	.58	.39

* P value between the RCC and sRVOT-p groups.

Data are presented as number (%) or mean ± standard deviation.

AAD = antiarrhythmic drugs, BSA = body surface area, GCV/AIV = great cardiac vein/anterior interventricular vein, LCC = left coronary cusp, LVEF = left ventricular ejection fraction, PVC = premature ventricular contraction, RCC = right coronary cusp, RLJ = RCC/LCC junction, RVOT = right ventricular outflow tract, sRVOT-a = anteroseptal RVOT, sRVOT-p = posteroseptal RVOT.

incidence of antiarrhythmic drug use ($P = .85$), daily PVC burden ($P = .41$), and sinus QRS axis ($P = .45$) also did not significantly differ between the groups.

3.2. ECG characteristics of RCC PVCs that differentiate from sRVOT PVCs

ECG characteristics of PVCs according to the site of origin are shown in Table 2. There were no significant differences in the R-wave ratio of leads II/III ($P = .15$) or the S-wave ratio of leads

aV_R/aV_L ($P = .11$) between groups. The R-wave duration ($81.4 ± 31.1$ vs $44.8 ± 7.0$, $48.2 ± 24.8$ ms, $P = .001$) and RWDI in lead V_1 and V_2 ($51.3 ± 22.0$ vs $31.2 ± 7.5$, $30.6 ± 15.4\%$, $P = .005$) were significantly longer in the RCC PVCs than the sRVOT PVCs. The ROC curve showed that a R-wave duration of $≥ 59$ ms predicted successful RCC ablation with 71% sensitivity and 89% specificity (AUC, 0.795; $P = .001$). The incidence of a predominantly positive lead I was significantly greater in the RCC PVCs than the sRVOT-p PVCs and sRVOT-a PVCs (100% vs 75%, 25% respectively; $P < .001$). The mean S-wave amplitude in lead

Table 2
ECG characteristics of PVCs, according to site of origin.

	RCC (n = 18)	sRVOT-p (n = 20)	sRVOT-a (n = 8)	P value	P value*
QRS axis (°)	20.6 ± 33.9	22.6 ± 32.6	22.6 ± 32.6	.45	.91
PVC QRSD, ms	156 ± 21	156 ± 22	151 ± 14	.57	.38
Precordial transition					
Sinus beat				.09	.03
V_1-V_2	6	2	4		
V_3	1	4	8		
V_4-V_6	11	2	8		
PVC				.11	.12
V_1-V_2	4	0	1		
V_3	11	4	9		
V_4-V_6	3	4	10		
BBB pattern				.28	.52
RBBB	3	0	1		
LBBB	15	8	19		
Positive lead I	18 (100)	15 (75)	2 (25)	<.001	.43
S amplitude in lead I (mV)	0.03 ± 0.05	0.06 ± 0.09	0.02 ± 0.2	<.001	.35
R amplitude in lead II (mV)	1.7 ± 0.9	1.7 ± 0.8	1.9 ± 0.7	.81	.99
R amplitude in lead III (mV)	1.3 ± 0.8	1.3 ± 0.4	1.8 ± 0.5	.07	.95
R amplitude lead II/III ratio	1.4 ± 0.8	1.4 ± 0.9	1.1 ± 0.4	.15	.84
S amplitude in aV_R (mV)	1.0 ± 0.5	0.7 ± 0.0	0.7 ± 0.3	.04	.22
S amplitude in aV_L (mV)	0.4 ± 0.3	0.5 ± 0.2	0.9 ± 0.4	.004	.91
S amplitude lead aV_R/aV_L ratio	2.0 ± 1.5	1.7 ± 0.6	1.6 ± 0.6	.11	.61
V_{1-2} R-wave duration, ms	81.4 ± 31.1	44.8 ± 7.0	48.2 ± 24.8	.001	.02
V_{1-2} RWDI (%)	51.3 ± 22.0	31.2 ± 7.5	30.6 ± 15.4	.005	.06
RSWAI (%)	28 ± 26	28 ± 22	27 ± 23	.89	.89
MDI	51 ± 8	52 ± 8	53 ± 11	.82	.79
V_2 transition ratio	1.3 ± 1.2	0.7 ± 0.4	0.6 ± 0.6	.09	.28

* P value between the RCC and sRVOT-p groups.

amp = amplitude, BBB = bundle branch block, GCV/AIV = great cardiac vein/anterior interventricular vein, LCC = left coronary cusp, MDI = maximum deflection index, RCC = right coronary cusp, RLJ = RCC/LCC junction, RSWAI = R/S-wave amplitude index, RVOT = right ventricular outflow tract, RWDI = R-wave duration index, sRVOT-a = anteroseptal RVOT, sRVOT-p = posteroseptal RVOT, VC = premature ventricular contraction.

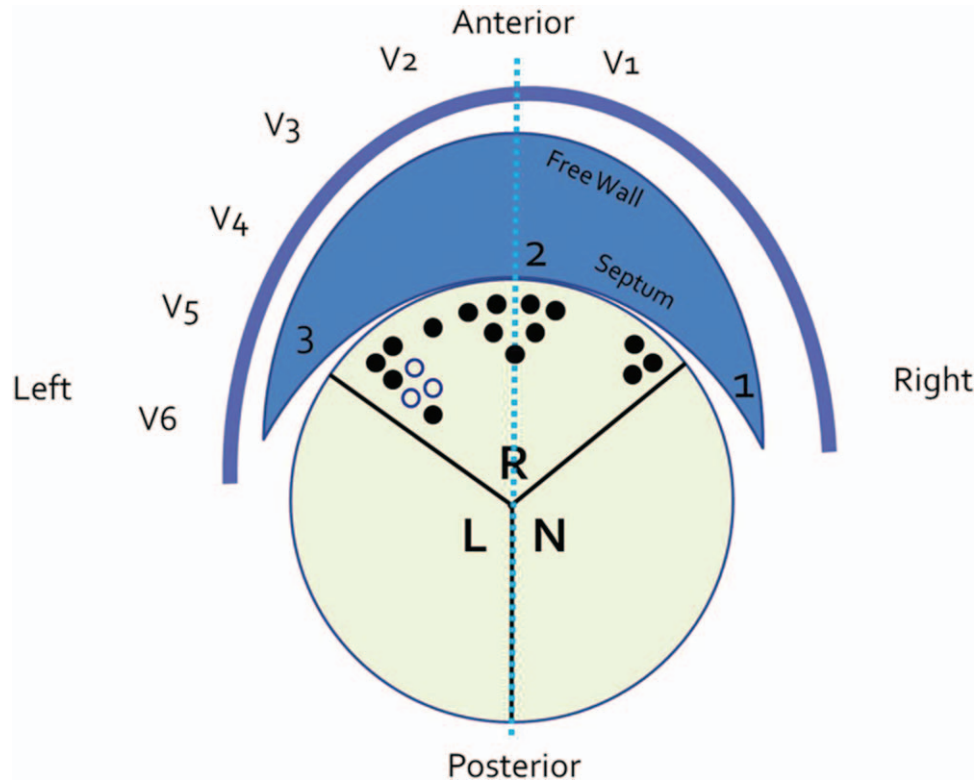


Figure 2. Distribution of successful RCC ablation sites. Three are posterior, 7 are middle, 1 is middle anterior, and 7 are anterior RVOT. a, anterior; L, left coronary cusp; m, middle; N, noncoronary cusp; p, posterior; R, right coronary cusp; RVOT, right ventricular outflow tract.

aV_R was significantly larger (1.0 ± 0.5 vs 0.7 ± 0.0 , 0.7 ± 0.3 mV, $P = .04$), whereas the mean S-wave amplitude in lead aV_L was significantly smaller in RCC PVCs than the sRVOT-p and sRVOT-a PVCs (0.4 ± 0.3 vs 0.5 ± 0.2 , 0.9 ± 0.4 mV, $P = .004$). There was a trend that the V_2 transition ratio was greater in the RCC PVCs than the sRVOT-p PVCs and sRVOT-a PVCs (1.3 ± 1.3 vs 0.7 ± 0.4 , 0.6 ± 0.5 , respectively; $P = .09$).

3.3. Electrophysiologic characteristics during mapping and RF ablation

Within the RCC, the successful ablation sites were 7 anterior, 7 middle, 1 middle anterior, and 3 posterior (Fig. 2). Among the 7 anterior RCC PVCs, 3 were ablated successfully under the valve in the RCC. Perfect pace mapping (≤ 10 mA, 2 ms) was found in 2 (11%) RCC patients and in 5 (27%) patients with other site of origins. Three of those 5 were in the sRVOT, and the other 2 were in the LCC-RCC junction. In 3 patients, RCC pacing capture was not possible, and in 5 patients, pacing capture was not evaluated at the sRVOT opposite the RCC. sRVOT ablation was performed in 15 of 18 RCC patients, and PVCs subsided transiently in 5 (33%) patients during sRVOT ablation. The pre-QRS time was significantly earlier in the successful RCC ablation sites (-38 ± 12 ms) than in the failed sRVOT sites (-22 ± 8 ms) ($P < .001$). The ROC curve showed that a pre-QRS time of ≥ -31 ms predicted successful RCC ablation with 67% sensitivity and 94% specificity (AUC, 0.867; $P < .001$) (Fig. 3). The total number of RF ablation applications was 9.8 ± 7.0 , including 3.7 ± 2.1 for the RCC sites and 5.8 ± 7.2 for the sRVOT sites (Table 3).

4. Discussion

Most idiopathic PVCs come from the outflow tract of both ventricles. ECG characteristics have been previously reported for the ASOV, including the LCC, RCC/LCC commissural junction,

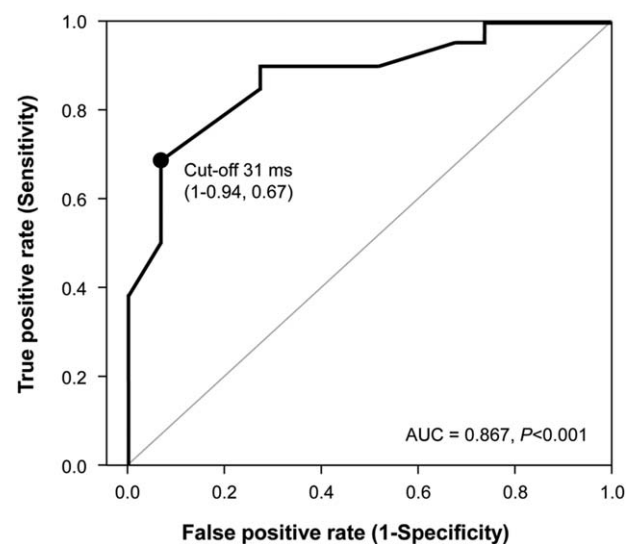


Figure 3. ROC curve analysis showing the predictive cut-off value of the pre-QRS time for successful RCC PVC RF ablation. PVC, premature ventricular contraction; RCC, right coronary cusp; RF, radiofrequency; ROC, receiver operating characteristic.

Table 3
Electrophysiological characteristics of the 18 RCC PVCs during mapping and RF ablation.

Patients	# 1	# 2	# 3	# 4	# 5	# 6	# 7	# 8	# 9	# 10	# 11	# 12	# 13	# 14	# 15	# 16	# 17	# 18
Pre-PVC QRS, ms																		
RCC	-16	-40	-28	-50	-45	-50	-21	-31	-30	-55	-45	-36	-35	-40	-30	-30	-49	-48
RVOT	-23	-25	-21	-30	-40	-26	-18	-21	-10	-	-	-	-30	-10	-14	-10	-30	-22
Pre-potential	+	-	-	-	-	-	-	-	-	+	-	-	+	-	-	-	-	-
Late potential-SR	-	-	-	-	-	-	-	-	-	+	-	-	+	-	-	-	-	-
Pace map score																		
RCC	poor	bad	nc	bad	bad	exc	bad	good	bad	nc	bad	poor	good	exc	good	good	bad	nc
RVOT	-	-	-	exc	-	bad	poor	exc	bad	-	-	-	bad	bad	bad	bad	exc	bad
HB potential-SR	+	-	-	-	-	-	-	-	+	-	-	-	+	-	-	-	-	-
No. of RF lesions	4	14	9	16	30	11	22	8	8	1	8	6	6	8	4	5	8	7
RCC	4	2	3	5	5	1	3	8	3	1	8	1	6	2	4	5	3	4
RVOT	0	12	6	11	25	10	18	0	5	0	0	5	0	0	0	0	4	3
RVOT ablation	-	+	+	+	+	+	+	-	-	-	-	-	-	-	-	-	+	-
PVC subside	-	+	+	-	+	+	+	-	-	-	-	-	-	-	-	-	-	-
Subside time (s)	-	30	10	-	40	30	15	-	-	-	-	-	-	-	-	-	-	-
Site within RCC	m	m	p	m	ma	a	m	a	a	m	m	a	p	a	m	p	a	a
Follow-up																		
Duration, months	25	21	36	9	32	26	25	55	38	29	30	52	36	11	38	13	40	13
Recurrence	N	N	N	N	N	N	N	N	N	N	N	N	N	N	N	N	N	N

a = anterior, exc = excellent, m = middle, ma = mid-anterior, ms = msec, N = none, nc = no capture, No = number, p = posterior, PVC = premature ventricular contraction, RCC = right coronary cusp, RF = radiofrequency, RVOT = right ventricular outflow tract, SR = sinus rhythm.

and epicardial sites.^[2-4,11-16] In our experience, many OT PVCs are difficult to differentiate from septal site RVOT and ASOV PVCs. In particular, there is a close and complex anatomical relationship between the RCC sites and the septal RVOT. This study attempted to determine the ECG and electrophysiological characteristics of RCC PVCs considering their anatomical relationship to the septal RVOT in order to successfully guide ablation procedures.

ECG measurements indicated that the bundle branch block pattern and the sites of precordial transition of the PVCs varied between RCC PVCs and PVCs of other sites of origin. Despite the variability in ECG morphology observed in successfully ablated RCC PVCs, the absence of a predominantly positive QRS in lead I, longer R-wave duration in lead V₁ and V₂, and greater V₁₋₂ RWDI and V₂ transition ratio suggest an unsuccessful ablation attempt in the RCC. A pre-QRS interval of more than -31 ms predicted a successful RCC ablation with 67% sensitivity and 94% specificity, even without perfect pace mapping.

The RCC site generally approximates the posterior septal aspect of the RVOT, whereas the anterior aspect of the RVOT tends to abut the LCC.^[17] Because of this arcing anatomy, the intimate nature of these 2 structures explains why pace maps from these distinct locations can be morphologically similar on surface ECGs. As a result, the RCC has less of an inferior axis relative to the sRVOT. The differences in the vectors may be explained by the more inferoposterior location of the RCC compared to the RVOT.^[17]

Classic ECG in patients with LVOT tachycardia has an RBBB morphology with a strong inferior axis evidenced by tall R-waves in leads II, III, and aV_F and QS complexes in aV_R and aV_L. Important variants of this classic ECG require a correlation with the underlying anatomy for interpretation. Because of the continuity between the posteroseptal RVOT and anterior LVOT, a very similar R-wave in lead V₁ is seen with arrhythmias that originate in either structure. The RCC is slightly more posterior than the posterior RVOT, and the R-wave amplitude is greater

when an arrhythmia originates from these structures. Lead I is typically positive with an origin on the right posterior side of the RVOT or RCC. Correlating the morphology in leads I and V₁ with the underlying anatomy can provide clarity.

Since both of these leads are superior and OT VT originates from a superior location, the vast majority of OT arrhythmias show simultaneously negative deflections in aV_R and aV_L leads. However, lead aV_L becomes less negative due to the anatomic location of the RCC region in the LVOT.^[15] Without exception, all OT arrhythmias exhibit positive deflection in leads II, III, and aV_F. The ratio of the positivity may yield clues regarding the location of the sites of origin. In the case of RCC PVCs, the location is slightly rightward and inferoposterior compared to LCC PVCs. The R-wave is higher in lead II than in lead III and has a less positive amplitude than that of the septal RVOT, but this difference is not significant.

In 90% of aortic root ventricular arrhythmias (VAs), a two-component electrogram with the earliest deflection preceding QRS onset of the VA was recorded at the successful ablation site. The first component of the electrogram (prepotential) was usually a smaller and higher frequency potential that preceded QRS onset, whereas the second component had a larger potential and occurred simultaneously with QRS onset. The mechanism of these prepotentials remains unclear; however, prepotentials may represent activation of myocardial fibers connecting the VAs origin to the breakout site or the VA origin itself. The second potential may represent the activation of the local myocardium at the breakout site. Ito et al^[18] reported that local ventricular activation at the successful ablation site on the left sinus valve preceded QRS onset by an average of -31 ± 10 ms.

In this study, the ECG and electrophysiological characteristics of RCC PVCs correlated with the results of the cardiac anatomy. These characteristics were useful for successful ablation of PVCs with an RCC site of origin. This has important implications for pre-procedural planning and appropriate patient counseling, and may help physicians increase successful outcomes in RCC RF

ablation. In our experience, many RCC PVC cases were first ablated from the RVOT or other sites with a perfect pace map, and as a result, we spent time ablating sRVOT sites. To the best of our knowledge, this is the first study to suggest useful ECG and electrophysiology characteristics for achieving successful RCC site ablation and avoiding unnecessary additional ablation at other sites.

The present study did have several limitations. First, this study was a single-center, retrospective study derived from a real world practice with inherent limitations. Hence the results of our study should be considered as hypothesis generating, and future prospective studies are warranted to confirm our results. As with any study involving the use of the 12-lead ECG, there are limitations due to variation in the anatomic orientation of the heart in relation to the placement of the ECG leads. Despite these limitations, surface ECG criteria may play an important role in the localization of PVCs in patients with idiopathic PVCs occurring in the absence of structural heart disease. We sought to minimize any potential factors that could influence surface ECG by including only patients with normal hearts. The use of intracardiac echocardiography to determine the catheter position also improved the accuracy of pace mapping in our series. Because only normal hearts were included, these criteria may not necessarily be useful in patients with a large scar burden or unusual anatomy, and caution must be exercised when interpreting ECG findings in these patient subgroups. Uncoiling of the aorta with increasing age results in a change in the angulation and orientation of the aortic valve, which could also affect ECG findings. Despite these limitations, we believe that these ECG characteristics represent an important tool in counseling patients with respect to the likely site of origin if the PVCs display a typical aortic cusp pattern, and will be helpful in guiding more detailed mapping and successful ablation.

In conclusion, the RCC is usually located opposite the septal RVOT. Despite the variability in the ECG morphology of successfully ablated RCC PVCs, the absence of a predominantly positive QRS in lead I, longer R-wave duration in lead V₁ or V₂, and greater V₁₋₂ R wave duration index suggests that effective ablation is unlikely. A pre-QRS time of more than -31 ms predicts successful RCC ablation with 67% sensitivity and 94% specificity, even without perfect pace mapping.

Acknowledgments

We wish to thank Se Hyun Kim and Hyung Sik Kim at Samsung Medical Center for their assistance and support with data collection.

Author contributions

Conception and coordination of the study: KM Park, SI Im. Design of ethical issues: YK On, JS Kim. Acquisition of data: HB Gwag, SH Lee, Y Park. Data review: SI Im, KM Park. Statistical analysis: SJ Park. Manuscript preparation: SI Im, KM Park. Manuscript approval: all authors.

References

- [1] Tada H, Ito S, Naito S, et al. Idiopathic ventricular arrhythmia arising from the mitral annulus: a distinct subgroup of idiopathic ventricular arrhythmias. *J Am Coll Cardiol* 2005;45:877-86.
- [2] Ouyang F, Fotuhi P, Ho SY, et al. Repetitive monomorphic ventricular tachycardia originating from the aortic sinus cusp: electrocardiographic characterization for guiding catheter ablation. *J Am Coll Cardiol* 2002;39:500-8.
- [3] Kanagaratnam L, Tomassoni G, Schweikert R, et al. Ventricular tachycardias arising from the aortic sinus of valsalva: an under-recognized variant of left outflow tract ventricular tachycardia. *J Am Coll Cardiol* 2001;37:1408-14.
- [4] Lin D, Ilkhanoff L, Gerstenfeld E, et al. Twelve-lead electrocardiographic characteristics of the aortic cusp region guided by intracardiac echocardiography and electroanatomic mapping. *Heart Rhythm* 2008;5:663-9.
- [5] Yamada T, Murakami Y, Yoshida N, et al. Preferential conduction across the ventricular outflow septum in ventricular arrhythmias originating from the aortic sinus cusp. *J Am Coll Cardiol* 2007;50:884-91.
- [6] Yamada T, Yoshida Y, Inden Y, et al. Idiopathic premature ventricular contractions exhibiting preferential conduction within the aortic root. *Pacing Clin Electrophysiol* 2010;33:e10-3.
- [7] Wang YB, Chu JM, Song SK, et al. [Preferential conduction to right ventricular outflow tract leads to left bundle-branch block morphology in patient with premature ventricular contraction originating from the aortic sinus cusp]. *Zhonghua Xin Xue Guan Bing Za Zhi* 2013;41:13-7.
- [8] Yamada T, Doppalapudi H, McElderry HT, et al. Idiopathic mitral annular PVCs with multiple breakouts and preferential conduction unmasked by radiofrequency catheter ablation. *Pacing Clin Electrophysiol* 2012;35:e112-5.
- [9] Yamada T, McElderry HT, Doppalapudi H, et al. Catheter ablation of ventricular arrhythmias originating in the vicinity of the His bundle: significance of mapping the aortic sinus cusp. *Heart Rhythm* 2008;5:37-42.
- [10] Mountantonakis SE, Frankel DS, Gerstenfeld EP, et al. Reversal of outflow tract ventricular premature depolarization-induced cardiomyopathy with ablation: effect of residual arrhythmia burden and preexisting cardiomyopathy on outcome. *Heart Rhythm* 2011;8:1608-14.
- [11] Hachiya H, Aonuma K, Yamauchi Y, et al. How to diagnose, locate, and ablate coronary cusp ventricular tachycardia. *J Cardiovasc Electrophysiol* 2002;13:551-6.
- [12] Bala R, Marchlinski FE. Electrocardiographic recognition and ablation of outflow tract ventricular tachycardia. *Heart Rhythm* 2007;4:366-70.
- [13] Bala R, Garcia FC, Hutchinson MD, et al. Electrocardiographic and electrophysiologic features of ventricular arrhythmias originating from the right/left coronary cusp commissure. *Heart Rhythm* 2010;7:312-22.
- [14] Daniels DV, Lu YY, Morton JB, et al. Idiopathic epicardial left ventricular tachycardia originating remote from the sinus of Valsalva: electrophysiological characteristics, catheter ablation, and identification from the 12-lead electrocardiogram. *Circulation* 2006;113:1659-66.
- [15] Berruezo A, Mont L, Nava S, et al. Electrocardiographic recognition of the epicardial origin of ventricular tachycardias. *Circulation* 2004;109:1842-7.
- [16] Bazan V, Gerstenfeld EP, Garcia FC, et al. Site-specific twelve-lead ECG features to identify an epicardial origin for left ventricular tachycardia in the absence of myocardial infarction. *Heart Rhythm* 2007;4:1403-10.
- [17] Asirvatham SJ. Correlative anatomy for the invasive electrophysiologist: outflow tract and supraventricular arrhythmia. *J Cardiovasc Electrophysiol* 2009;20:955-68.
- [18] Ito S, Tada H, Naito S, et al. Development and validation of an ECG algorithm for identifying the optimal ablation site for idiopathic ventricular outflow tract tachycardia. *J Cardiovasc Electrophysiol* 2003;14:1280-6.